Regulation of human *PTCH1b* expression by different 5' untranslated region *cis*-regulatory elements

Petar Ozretić[1], Alessandra Bisio[2], Vesna Musani[1], Diana Trnski[1], Maja Sabol[1], Sonja Levanat[1,*], and Alberto Inga[2]

[1]Laboratory for Hereditary Cancer; Division of Molecular Medicine; Ruđer Bošković Institute; Zagreb, Croatia; [2]Laboratory of Transcriptional Networks; Center for Integrative Biology; University of Trento; Mattarello, Trento, Italy

PTCH1 gene codes for a 12-pass transmembrane receptor with a negative regulatory role in the Hedgehog-Gli signaling pathway. *PTCH1* germline mutations cause Gorlin syndrome, a disorder characterized by developmental abnormalities and tumor susceptibility. The autosomal dominant inheritance, and the evidence for *PTCH1* haploinsufficiency, suggests that fine-tuning systems of protein patched homolog 1 (PTC1) levels exist to properly regulate the pathway. Given the role of 5' untranslated region (5'UTR) in protein expression, our aim was to thoroughly explore *cis*-regulatory elements in the 5'UTR of *PTCH1* transcript 1b. The (CGG)$_n$ polymorphism was the main potential regulatory element studied so far but with inconsistent results and no clear association between repeat number and disease risk. Using luciferase reporter constructs in human cell lines here we show that the number of CGG repeats has no strong impact on gene expression, both at mRNA and protein levels. We observed variability in the length of 5'UTR and changes in abundance of the associated transcripts after pathway activation. We show that upstream AUG codons (uAUGs) present only in longer 5'UTRs could negatively regulate the amount of PTC1 isoform L (PTC1-L). The existence of an internal ribosome entry site (IRES) observed using different approaches and mapped in the region comprising the CGG repeats, would counteract the effect of the uAUGs and enable synthesis of PTC1-L under stressful conditions, such as during hypoxia. Higher relative translation efficiency of *PTCH1b* mRNA in HEK 293T cultured hypoxia was observed by polysomal profiling and Western blot analyses. All our results point to an exceptionally complex and so far unexplored role of 5'UTR *PTCH1b cis*-element features in the regulation of the Hedgehog-Gli signaling pathway.

Introduction

The Hedgehog-Gli (Hh-Gli) pathway is a highly conserved cellular mechanism for transducing signals from the cell surface into the nucleus, stimulating expression of many genes that result in an appropriate physiological response to changes in the cellular environment.[1] Because of its important role in many developmental processes, several human syndromes involving congenital malformations, are caused by genetic alterations of Hh-Gli pathway genes.[2] In the last decades, the greatest interest of both scientific research and pharmaceutical industry has been on exploration of Hh-Gli pathway's connection with cancerogenesis in an increasing number of tumor types.[3] The basic members of Hh-Gli pathway include the Hh family of 3 ligands coded by Sonic (*SHH*), Indian (*IHH*) and Desert (*DHH*) Hedgehog genes.[4] Hedgehog proteins (HH) are secreted from different

tissues at various developmental stages and all 3 trigger a signaling cascade in target cells by binding to the 12-pass transmembrane receptor protein patched homolog 1 (PTC1), which relieves its catalytic inhibition of the G-protein-coupled receptor-like signal transducer Smoothened homolog (SMO).[5,6] De-repression of SMO triggers a cascade of downstream events in primary cilia, which ends in the activation of glioma-associated oncogene family of zinc finger transcription factors GLI1, GLI2 and GLI3 that initiate transcription of Hh-Gli target genes.[7–9] The outcome of activated Hh-Gli signaling depends on the signal-receiving cell, and can include an overexpression of a variety of cell-specific transcription factors which mediate different developmental fate responses like cell proliferation, expression of anti-apoptotic proteins, angiogenesis, and epithelial-to-mesenchymal transition.[10] One of Hh-Gli target genes is *GLI1* itself, which further amplifies the signal resulting in a positive feedback

loop.[11] Other Hh-Gli target genes code for PTC1 and Hedgehog-interacting protein (HHIP) that can also bind HH, mediating a negative feedback loop by limiting the quantity of available unbound ligand required for pathway activation.[11–13]

The human *PTCH1* gene (MIM 601309) is located on chromosome 9q22.32 and spans about 74 kilobases.[14] There are at least 7 major *PTCH1* transcript variants with 24 exons, of which 23 are coding, and with the first exon being specific for each variant.[15–17] Those 7 transcripts code for 4 different PTC1 isoforms with different N-terminal region. Functional analyses have revealed that alternative first exons affect protein isoform stability, expression pattern, as well as their ability to inhibit SMO.[15–18] Transcript 1b and its product isoform L, the largest PTC1 protein with the highest repressing activity on SMO, are considered as the canonical transcript and protein. The expression of the transcript 1b is specifically induced in nodular basal cell carcinoma (BCC).[15,19] Transcripts 1b and 1c harbor in their promoter one active Gli-consensus binding site, which upon HH stimulation affects their specific expression.[20]

The *PTCH1* gene is suggested to be a tumor suppressor, and inactivating germline mutations of *PTCH1* cause basal cell nevus syndrome (BCNS) (MIM 109400).[21,22] BCNS or Gorlin syndrome is an uncommon autosomal dominant inherited disorder, which is characterized by multiple skeletal, dental, ophthalmic, and neurological abnormalities, and predisposition for developing multiple basal cell carcinomas (BCC).[23] Most of the malformations are caused by *PTCH1* haploinsufficiency, indicating that the physiological pathway activity is sensitive to relatively small changes in PTC1 levels.[19,24]

One of the main roles of 5′ untranslated region (5′UTR) of mRNAs is post-transcriptional regulation of gene expression, starting from the initiation of protein translation.[25–27] The 5′UTRs can differ in length, nucleotide content, secondary structures, and the presence of different functional elements.[28] The main regulatory elements in 5′UTRs are secondary structures, including internal ribosome entry sites (IRESes), upstream open reading frames (uORFs) and upstream AUG codons (uAUGs), as well as binding sites for RNA-binding proteins.[29] These *cis*-regulatory elements can affect the stability or translational efficiency of mRNAs, resulting in a rapid alteration of protein level in response to internal and external stimuli, without the need for new mRNA synthesis.[30] So far, many diseases are associated to improper functioning, caused for example by point mutations, of any of the 5′UTR *cis*-regulatory elements mentioned above.[31]

Reports differ on the *PTCH1b* 5′UTR length: in the NCBI GenBank it is annotated as 188-nucleotide long (RefSeq ID NM_000264.3), while in Ensembl it includes additional 112 nucleotides upstream, for a total length of 300 nucleotides (Transcript ID ENST00000331920.6). Even longer *PTCH1b* 372 nucleotides long 5′UTR was reported.[20] Up to now, the only studied potential regulatory element has been a $(CGG)_n$ repeat polymorphism present immediately upstream the AUG start site, but not clear association between repeat numbers and disease risk was found.[32,33] Here we thoroughly explored *cis*-element features of the 5′UTR of the *PTCH1* transcript 1b applying the methodology previously used for the functional analysis of 5′UTR of the *CDKN2A* gene.[34]

Results

The length of *PTCH1b* 5′UTR but not the number of CGG repeats has a dramatic impact on gene expression

To evaluate the effect of the CGG-repeat polymorphism and the different size of *PTCH1b* 5′UTR on the expression of an associated coding sequence, a series of reporter plasmids were constructed harboring 5, 7 or 8 CGG repeats in the context of a 188nt or 300nt long 5′UTR. These repeat numbers were all found in healthy, control population.[35]

Results of luciferase assays performed in transfected HCT116 $^{p53+/+}$ cells showed that the insertion of *PTCH1b* 5′UTR caused significant changes in Firefly luciferase (Fluc) activity compared to the empty plasmid (pGL3-P, based on the pGL3-Promoter Luciferase Reporter Vector) ($P < 0.0001$). The 188nt-long 5′UTR caused on average more than 2-fold increase in activity, while all alleles of the 300nt-long 5′UTR decreased luciferase activity around 5-fold. The CGG-repeat number showed some effect only in the context of 188nt-long 5′UTR, where the $(CGG)_5$ allele led to a slight increase in activity compared to both $(CGG)_7$ and $(CGG)_8$ alleles (**Fig. 1A**).

Results were similar in transfected MCF7 cells (**Fig. 1B**), although the 188nt-long 5′UTR caused on average more than 7-fold increase in Fluc activity, and the 300nt-long 5′UTR decreased Fluc activity of about 2-fold for $(CGG)_5$ and $(CGG)_8$ alleles. The CGG-repeat number showed a subtle impact in the context of the 188nt-long 5′UTR, with the $(CGG)_5$ allele being slightly more active compared to both $(CGG)_7$ and $(CGG)_8$ alleles (**Fig. 1B**). In the third cell line used, HEK 293T, results were comparable in pattern and level of gene reporter changes to those obtained in HCT116 cells (**Fig. 1C**).

PTCH1b 5′UTR sequences lead to higher levels of reporter transcript

To evaluate whether the results of luciferase assays are related to transcriptional or post-transcriptional effect of *PTCH1b* 5′UTR insertion, we quantified the relative levels of Fluc mRNA from the various transfected constructs. In HCT116 $^{p53+/+}$ cells, Fluc mRNA quantification showed that the presence of *PTCH1b* 5′UTR caused a significant increase in Fluc transcripts levels compared to the control pGL3-P plasmid ($P < 0.0001$). In contrast to the results of the reporter enzymatic activity, the 300nt-long 5′UTR resulted in equivalent or even higher increase in luciferase mRNA levels. The CGG-repeat number showed no impact on luciferase mRNA levels (**Fig. 1D**). Hence, the dramatic difference in reporter activity associated with the different *PTCH1b* 5′UTR length could be associated to post-transcriptional regulation.

Results were very similar in MCF7 and HEK 293T cells. The CGG-repeat number showed an impact in the context of 188nt-long 5′UTR, with $(CGG)_5$ allele resulting in higher Fluc transcript levels which was consistent with the results of luciferase assays (**Fig. 1E and F**). In HEK cells the $(CGG)_7$ allele led to higher Fluc mRNA levels compared to the $(CGG)_8$ allele in the 300nt-long 5′UTR construct (**Fig. 1F**).

The ratio between induction of luciferase activity and of transcript levels for the 188nt-long *PTCH1b* 5′UTR alleles in the
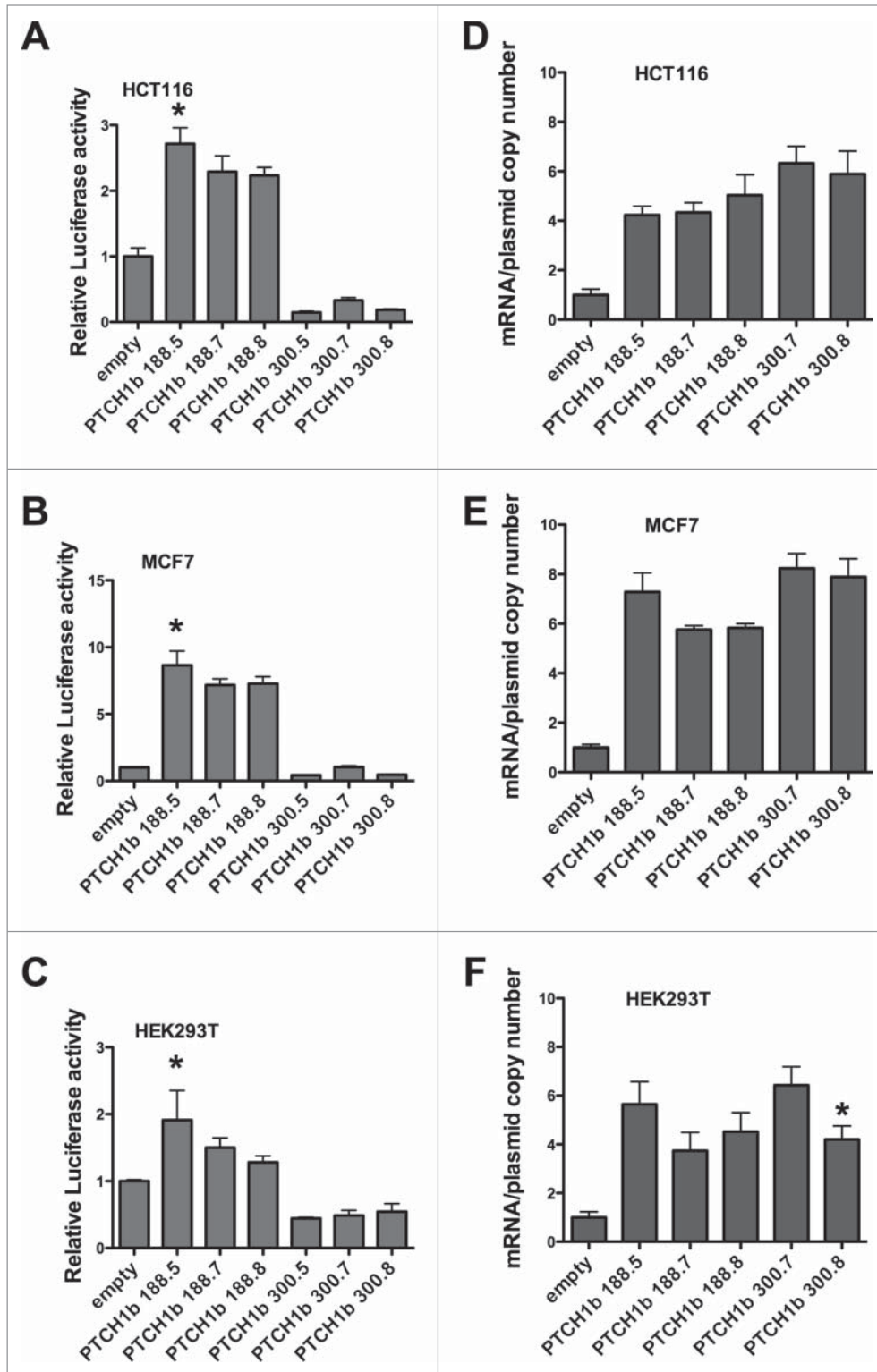
Figure 1. Impact of *PTCH1b* 5′UTR size and CGG-repeat number in gene reporter assays. pGL3-Promoter-derived constructs containing *PTCH1b* 5′UTRs (188 or 300 nucleotides) fused to the Firefly luciferase (Fluc) were transiently transfected in HCT116 $^{p53+/+}$ (**A**), MCF7 (**B**) and HEK 293T cells (**C**). Presented are the average fold inductions relative to the empty vector and standard deviations of at least 3 biological replicates. The luciferase values are expressed relative to the value obtained with an empty control vector. The same constructs were used to measure relative Fluc mRNA transcript levels in transiently transfected HCT116 $^{p53+/+}$ (**D**), MCF7 (**E**) and HEK 293T cells (**F**). Presented is the average Fluc mRNA expression normalized for the average plasmid copy number and for relative cDNA synthesis efficiency as revealed by the amplification of GAPDH and B2M mRNAs. For each UTR size type, results were compared to the corresponding reference allele with (CGG)$_7$; *P < 0.05

comparison with the control pGL3-P plasmid was around 1.0 for MCF7 cells, but lower for HCT116 and HEK 293T cells (around 0.6 and 0.4, respectively) (data not shown), suggesting that translation of an mRNA containing the 188nt-long *PTCH1b* 5'UTR is somewhat more efficient in MCF7 cells in comparison to the other 2 cell lines.

While developing these assays we identified a $(CGG)_6$ *PTCH1b* allele in one ovarian cancer patient.[35] Hence we constructed an additional pGL3-P-based plasmid harboring the 188nt- 5'UTR $(CGG)_6$ repeats and tested it in MCF7 and HEK 293T cells (**Fig. S1**). In MCF7 cells the $(CGG)_6$ allele gave 30−50% higher activity compared to the other alleles, but these results were not confirmed in HEK 293T cells.

The dramatic reduction in reporter gene activity observed with the 300nt-long *PTCH1b* 5'UTR is caused by uORF and uUAG

Given the previous reports that the *PTCH1b* 5'UTR can be up to 372nt long, we inspected this sequence for the presence of potential *cis*-regulatory elements. ATGpr and NetStart 1.0 tools predicted 2 uORFs and one uAUG codon within the 372nt and 300nt but not the 188nt long 5'UTR sequence (**Fig. 2A**).[36,37] The uORF1 and uORF3 share the same UGA stop codon positioned upstream from the *PTCH1b* canonical AUG, while the ORF from uAUG2 would span beyond the *PTCH1b* canonical AUG and under a different coding frame. Translation from uAUG2 would code for an 88 amino acid long peptide, but BLASTx analysis didn't find any known protein potentially translated from the predicted *PTCH1b* uORFs.[38]

To test the impact of the identified uAUGs in the gene reporter assays, we constructed 2 point mutations within the 300nt-long *PTCH1b* 5'UTR $(CGG)_7$ allele (c.-248G>T and c.-242A>T) abolishing uAUG2 and uAUG3, whose predicted ORFs obtained the highest *in silico* probability scores (data not shown). Luciferase assay in MCF7 and HEK 293T cells showed that the introduced mutations restored the activity of the reporter gene to levels equal to that of the corresponding 188nt allele vector, while not impacting on the relative transcript levels (**Fig. 2B and C**). For MCF7 cells we also included in the analysis a plasmid containing the 372nt long 5'UTR $(CGG)_7$ construct. Computational analyses did not find additional regulatory elements within those additional 72 nucleotides. This construct led to a reduction in reporter activity compared to the empty vector, similar to the results obtained with the wild type 300nt long 5'UTR. Given that these UTRs would differ only for the transcription start sites, the entire sequence of the 188nt UTR is included in the 300nt UTR, while the 372nt UTR is an extension to the 5' of the 300nt 5'UTR (**Fig. 2A**).

The *PTCH1b* transcript with the shorter 5'UTR is preferentially induced after Hedgehog-Gli pathway activation

Since we showed that *PTCH1b* 5'UTR length strongly affect the translation efficiency of the downstream coding sequence, we wanted to inspect if these 2 *PTCH1b* 5'UTR transcripts exist and, in case, at which relative ratio in cell lines. We also wanted to inspect if conditions mimicking an active Hh-Gli pathway

preferentially increases the expression of short (188nt) or long (300nt, or potentially 372nt) *PTCH1b* 5'UTRs. Quantification of *PTCH1b* mRNAs containing at least a 188nt- or at least a 300nt-long 5'UTR was performed by qPCR under basal condition and upon GLI1 overexpression in HCT116 $^{P53+/+}$ and MCF7 cells. In both cell lines the longer transcript(s) was virtually exclusive in basal conditions and appeared to be still the most abundant after pathway activation ($P < 0.0001$), although the 188nt-long 5'UTR transcript appeared also to be induced (**Fig. 3**). It was also apparent that GLI1 overexpression led to much higher *PTCH1b* induction in MCF7 breast cancer cells compared to HCT116 $^{P53+/+}$ cells.

PTCH1b 5'UTR can mediate cap-independent translation, regardless of 5'UTR size and CGG-repeat number

Several features such as high GC-content, relative long size, potentially highly structured conformation and presence of uORFs and uAUG, led us to hypothesize that *PTCH1b* 5'UTR could affect the efficiency of ribosome loading and scanning during cap-dependent initiation of PTC1-L translation. This might even anticipate that *PTCH1b* 5'UTR possesses the ability to modulate translation initiation from the internal canonical PTC1-L AUG in cap-independent manner. To test this assumption, we decided to construct bicistronic dual-luciferase vectors (pRuF) with *PTCH1b* 5'UTR cloned as intervening sequence between *Renilla* (Rluc) and Firefly luciferase (Fluc) reporter genes.

Results of luciferase assays in MCF7 cells showed that the *PTCH1b* 5'UTR caused significant increase in Fluc relative to Rluc activity compared to a control (empty) pRuF plasmid ($P < 0.0001$). Notably both size types (188nt and 300nt) led to equivalent results and there was no effect due to the CGG repeat number. Interestingly, the levels of increase in Fluc activity with the *PTCH1b* 5'UTR constructs were similar to the activity of a pRuF plasmid containing the 5'UTR of the c-MYC gene that is known to act as a cellular internal ribosome entry site (**Fig. 4A**).[39] The fact that in the bicistronic vectors we did not observe a negative impact of the uAUGs present in the 300nt 5'UTR is consistent with the cap-independent nature of Firefly luciferase translation and suggest direct ribosome loading downstream from those AUGs.

Results of dual luciferase assays were nearly identical in HEK 293T cells, except for a lower magnitude of relative Fluc induction, on average a 4.5-fold increase, and a slightly higher activity of the c-MYC 5'UTR. A trend for somewhat higher Fluc activity with higher number of CGG repeats was apparent and statistically significant for the 300nt $(CGG)_8$ compared to both $(CGG)_5$ and $(CGG)_7$ alleles, but the biological relevance of this observation cannot be anticipated (**Fig. 4C**).

The observed higher Fluc activity could in principle also be due to the production of an additional transcript containing only the Fluc reporter, which would originate from a cryptic promoter activity within *PTCH1b* 5'UTR and be translated in a cap-dependent manner. Therefore, we performed qPCR experiments to measure the relative amounts of Rluc and Fluc mRNA regions. A relative ratio of Fluc to Rluc mRNA equal to one would
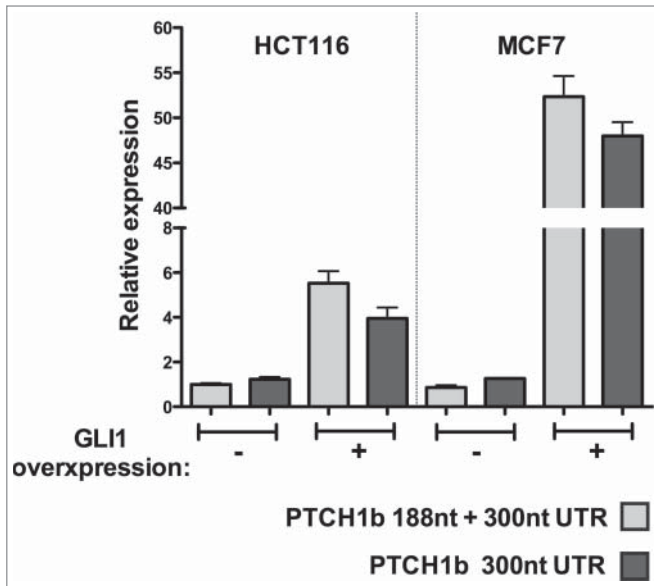
A

372nt PTCH1b 5'UTR

5'...gggaccgcaaggagugccgcggaagcgcccgaaggacaggcucgcucggcgcgc
cggcucucgcucuuccgcgaacugg**aug¹**ugggcagcggcggccgcagagaccucgg
gaccccgcgca**aug²**uggca**aug³**gaaggcgcagggucugacuccccggcagcggcc
gcggccgcagcggcagca**g**cgcccgccgug**uga¹,³**gcagcagcagcggcuggucuguc
aaccggagcccgagcccgagcagccugcggccagcagcguccucgcaagccgagcgcc
caggcgcgccaggagcccgcagcagcggcagcagcgcgccgggccgcccgggaagccu
ccguccccgcggcggcggcggcggcggcggcaac**AUG**GCCUCGGCUGG<u>UAA²</u>...3'

uORF¹,³: **aug¹**(M)WAAAAAETSGPPRNVA**aug³**(M)EGAGSDSPAAAAAAAAAAPAV*uga¹,³*

uORF²:**aug²**(M)WQWKAQGLTPRQRPRPQRQQRPPCEQQQRLVCQPEPEPEQPAAS
SVLASRAPRRARSPQQRQQRAGPPGKPPSPRRRRRRRQHGLGW*UAA²*

B MCF7 HEK293T

Fold of Induction

empty, PTCH1b 188.7, PTCH1b 300.7, PTCH1b 300.7SDM, PTCH1b 372.7, empty, PTCH1b 188.7, PTCH1b 300.7, PTCH1b 300.7SDM

C MCF7 HEK293T

mRNA/plasmid copy number

empty, PTCH1b 188.7, PTCH1b 300.7, PTCH1b 300.7SDM, PTCH1b 372.7, empty, PTCH1b 188.7, PTCH1b 300.7, PTCH1b 300.7SDM

Figure 2. The 300- and 372nt-long *PTCH1b* 5'UTRs harbors upstream AUG codons (uAUGs) and open reading frames (uORFs) that impact on associated mRNA translation. (**A**) Shown is the human sequence of the *PTCH1b* 5'UTR starting from the 5' portion of the longest reported 372-nucleotide sequence. Three uAUGs (bold and numbered in superscript) are present in the 2 longer sized 5'UTRs. Two of these uAUG would form short uORFs consisting in 40 and 23 codons and sharing the same stop codon (underlined and numbered in superscript) in the 5'UTR. The second uAUG from the 5' end would instead form a longer ORF (89 codons in size), whose stop codon is in the *PTCH1b* coding sequence and in a different frame (upper case). Starting from 5', arrows mark the beginning of the 372nt, 300nt and 188nt UTR sequence. Hence, the 188nt UTR sequence is included in its entirety in the longer UTRs. (**B, C**) Introduction of 2 point mutations (c.-248G>T and c.-242A>T) into pGL3-P-type plasmid harboring 300nt long *PTCH1b* 5'UTR abolishing uAUG¹ and uAUG³ restored luciferase activity to levels comparable to the activity of the plasmid containing the 188nt long 5'UTR (**B**), with no impact on reporter gene transcription (**C**). The 372nt 5'UTR behaved similarly to the 300nt one in the reporter and mRNA quantification tests.

support the lack of a cryptic promoter activity for *PTCH1b* 5'UTR sequence, when inserted into the intercistronic region of the pRuF vector.

In MCF7 cells, Fluc to Rluc mRNA ratios for pRuF plasmids with 188nt-long 5'UTR harboring (CGG)$_5$ allele and 300nt-long 5'UTR harboring (CGG)$_7$ allele were slightly (30 to 40%) but significantly higher than 1.0 ($P < 0.0001$) (**Fig. 4B**). This could potentially indicate that for these 2 plasmids a cryptic promoter was created with *PTCH1b* 5'UTR insertion. However, since the Fluc activity for those 2 plasmids didn't differ compared

Figure 3. Quantification of 188- and 300-nucleotide long 5'UTRs from the endogenous *PTCH1b* gene. Analyses were conducted in HCT116 p53+/+ and MCF7 cancer cell lines, under basal culture conditions or 48 hours after ectopic GLI1 overexpression. In both cell lines GLI1 over-expression led to induction of *PTCH1b* expression, much stronger in MCF7 cells. The relative expression of transcripts containing a 5'UTR of at least 188nt or of at least 300nt in length was calculated using the ΔCt method and *GAPDH* plus *B2M* as reference genes (see **Materials and Methods**). The relative expression of the amplicon detecting all 5'UTR sizes (indicated as 188nt + 300nt) in HCT116 cells from control cultures was set to 1. Results plot the average relative expression and the standard deviation of 3 replicates.

to the other *PTCH1b* 5'UTR pRuF-type plasmids (**Fig. 4A**), and given that the mRNA quantification showed at best a 40% increase in Fluc/Rluc mRNA ratio while the reporter activity increased at least 8 fold, the involvement of a cryptic promoter is not likely. The relative ratio of Fluc to Rluc mRNA for all *PTCH1b* 5'UTR pRuF-type plasmids in HEK 293T cells was not significantly different from 1.0 ($P = 0.225$) (**Fig. 4D**). These results ruled out the presence of a potential cryptic promoter within *PTCH1b* 5'UTR inserts, and indicate that the higher activity of Fluc in luciferase assays in same cells arose from Fluc translated from a bicistronic pRuF mRNA in a cap-independent manner.

The first 76 nucleotides upstream the canonical AUG of the *PTCH1b* 5'UTR were previously predicted to share structural similarity with a common RNA motif involved in internal ribosome loading and initiation of translation of cellular mRNAs.[40] For a more precise mapping of the putative *PTCH1b* IRES motif, we constructed 3 additional pRuF-type plasmids: one preserving just those 76 nucleotides (*PTCH1b* IRES) and 2 by deleting them from either 188- or 300nt-long *PTCH1b* 5'UTR with 7 CGG repeats.

Based on results in MCF7 and HEK 293T cells, removing the putative IRES motif from pRuF with 188nt-long *PTCH1b* caused a significant decrease in Fluc activity, more pronounced in HEK cells, while removing those nucleotides from 300nt-long

PTCH1b 5'UTR caused an even larger decrease in activity (**Fig. 5A and C**). The plasmid containing only the putative *PTCH1b* motif achieved ~50% of the activity obtained by pRuF plasmids with either size of 5'UTR, indicating that the 76nt proximal region alone is not responsible for the entire IRES-like activity.

The bicistronic nature of the reporters' transcript produced by pRuF vectors with the *PTCH1b* deletion construct was investigated by qPCR. In both MCF7 and HEK 293T cells, although the relative Fluc/Rluc mRNA ratio for some pRuF-type plasmids differed in pairwise comparisons depending on CGG repeat numbers and UTR length ($P = 0.009$ and $P = 0.041$, respectively), none of them was significantly different from the results obtained with the control vector (**Fig. 5 B and D**). These results indicated that the decreased Fluc activity likely arose from reduced translation of the Fluc coding sequence.

To rule out alternative splicing event which could originate a monocistronic capped Fluc mRNA as another underlying mechanism for the increase in Fluc activity, unrelated to cap-independent translation, an RT-PCR approach was performed (**Fig. S2A**). Results indicated that both reporters were part of a single transcript and that no shorter transcripts variants containing Fluc were apparent (**Fig. S2B and C**). The two very closely spaced bands visible in the left panel are processed and un-processed transcripts, respectively.

Taken all the results with pRuF-type plasmids collectively, we propose that the *PTCH1b* 5'UTR can act as a cellular IRES, at least when ectopically placed in a bicistronic reporter construct.

Hypoxia can stimulate *PTCH1b* 5'UTR-mediated cap-independent translation

To begin exploring which cellular stress condition(s) could activate the initiation of protein translation controlled by the putative *PTCH1b* IRES motif, we drew upon previous findings that hypoxic conditions activate Hh-Gli pathway.[41,42] Hypoxic culture conditions for MCF7 cells transfected with pRuF plasmids caused a significant increase in Fluc activity for the plasmids harboring either c-MYC or *PTCH1b* 5'UTR, but not when the putative *PTCH1b* IRES motif was deleted (**Fig. 6**, left panel). Hypoxia also showed significant effects on Fluc activity in transfected HEK 293T cells ($P < 0.0001$) but surprisingly, in these cells hypoxia caused a decrease in Fluc activity and only for plasmids harboring either c-MYC or *PTCH1b* IRES motif, while there was no impact with the 2 deletion constructs lacking the proximal 76 nucleotides (**Fig. 6**, right panel).

The endogenous *PTCH1b* mRNA exhibits high relative translation efficiency in HEK 293T cells overexpressing GLI1 and during hypoxia

HEK 293T cells were transfected with a GLI1 overexpression, or a control vector. 24 hours post-transfection cells were placed in hypoxic chamber, or kept in normoxic growth conditions, for additional 16 hours. Cells were then processed for total RNA extraction or for sucrose gradient fractionation of cytoplasmic lysates followed by separation of polysomal or subpolysomal mRNAs (see **Materials and Methods** for details). Cells subjected
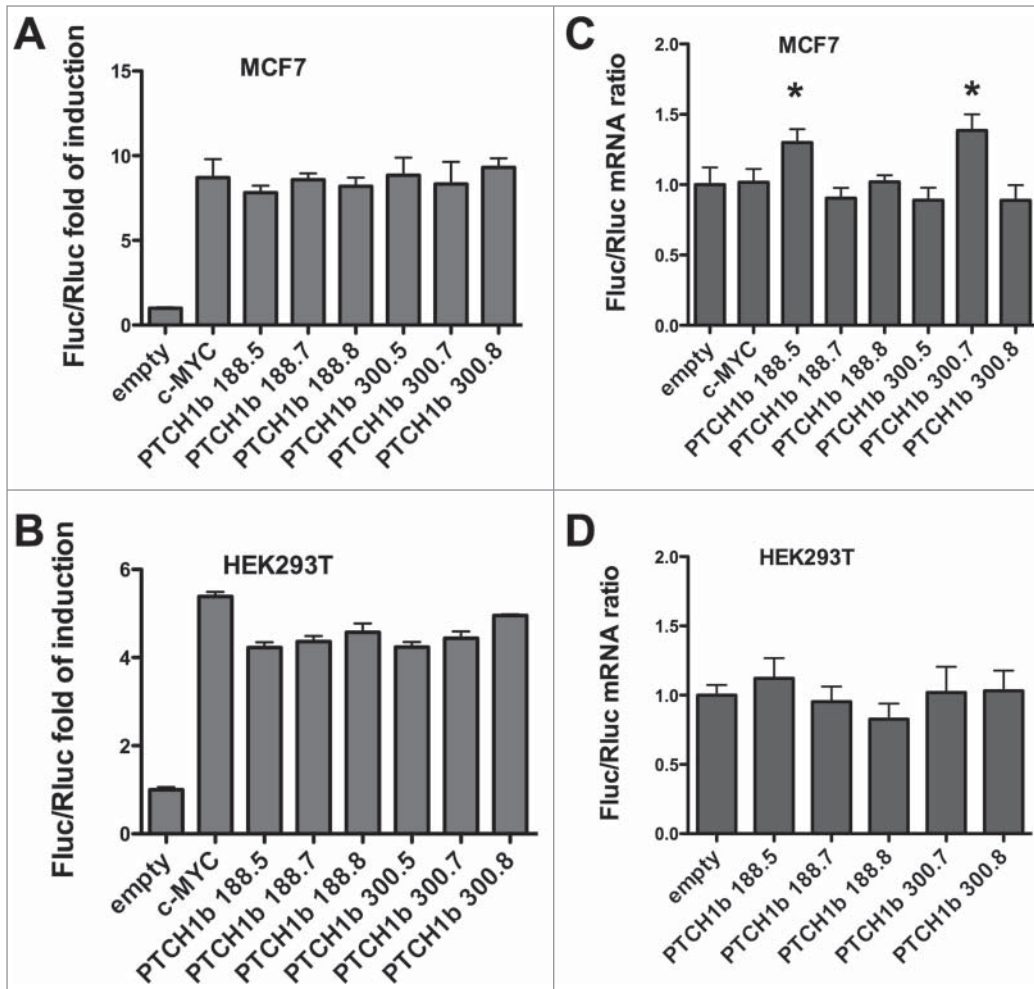
Figure 4. Impact of *PTCH1b* 5'UTR size and CGG-repeat number on cap-independent translation. Bicistronic pRuF-derived constructs were used to study the potential of the *PTCH1b* 5'UTR to drive cap-independent translation of the Firefly luciferase gene in transiently transfected MCF7 (**A**) or HEK 293T cells (**B**). Presented are the average ratios and standard deviations between Firefly (Fluc) and *Renilla* luciferase (Rluc) relative light units, normalized with the results obtained for empty pRuF vector, and standard deviation of at least 3 replicates. The *PTCH1b* 5'UTR size and CGG-repeat number are indicated. (**C, D**) The bicistronic nature of the transcript expressed by pRuF constructs was estimated measuring the Fluc/Rluc mRNA ratio by a qPCR approach. A ratio equal to 1.0 would strongly argue against the presence of a cryptic promoter within cloned *PTCH1b* 5'UTR resulting in a monocistronic Fluc mRNA transcript. A pRuF-type plasmid with cloned c-MYC 5'UTR was used as a positive control. For each UTR size type, results were compared to the corresponding reference allele with (CGG)$_7$; *P $<$ 0.05

polyribosomes indicated that large majority *PTCH1b* mRNAs are in active translation in HEK 293T cells cultured in normal medium (**Fig. 7B**). The GLI1 expression vector led to an increase in the *PTCH1b* mRNA and in its relative association with polysomes. No apparent difference in translation efficiency can be estimated for *PTCH1b* transcript containing the 188nt or 300nt long 5'UTR as virtually all the mRNAs appear to be containing a 5'UTR of at least 300nt, based on the relative expression obtained with the 2 primer pairs of which one is selective for transcript containing *PTCH1b* 5'UTR longer than 188 nucleotides. The reduction in *PTCH1b* mRNA in hypoxia seen at the level of total mRNA, was confirmed by polysomal analysis but was associated to a relatively small change in the distribution of the mRNA pool between polysomal and subpolysomal fractions, compared to the *PCNA* mRNA. This effect was particularly evident for GLI1 overexpressing cells. The ratio between polysomal and subpolysomal mRNAs is used as an estimate of relative translation efficiency (**Fig. 7C**). Similar to what

to the same treatments were collected for total protein extraction, while the effect of hypoxia on global protein synthesis was also measured. Results indicated that the *PTCH1b* mRNA containing 300nt long 5'UTR was the most prevalent transcript expressed in HEK 293T cells and its expression was induced by the transfection with a GLI1 overexpression plasmid (**Fig. 7A**). Hypoxia treatment led to a near 50% reduction in the relative expression of *PTCH1b* mRNA, which was not apparent in the GLI1 overexpression condition. GLI1 plasmid had no impact on relative *c-MYC* levels, which were also unaffected by the hypoxic culture condition, while *PCNA* mRNA showed about 50% reduction in hypoxia.

Relative quantification of cytoplasmic mRNAs associated (POL = polysome bound) or not (SUB = subpolysomal) with

was observed for *PTCH1b*, the *c-MYC* mRNA also showed similar polysomal versus subpolysomal distribution in the comparison between normoxia and hypoxia culture conditions (**Fig. 7B**). A slight increase in *PCNA* total mRNA observed in GL1 overexpressing cells cultured in hypoxia (**Fig. 7A**) was not associated with an increase in polysome association.

The effect of hypoxia on global protein synthesis was quantified by measuring non-radioactive methione-analog incorporation using a high-content imaging system (see **Materials and Methods**). About a 50% decrease in protein synthesis was observed in cells cultured in hypoxia (**Fig. 7D**). Despite the global decrease in protein synthesis, and consistent with the polysomal mRNA analysis, PTC1-L relative protein levels did not decrease in hypoxia, compared to normoxia and were higher in

cells transfected with the GLI1 overexpression construct (**Fig. 7E**). Collectively, these results are consistent with *PTCH1b* mRNA retaining high relative translation efficiency in conditions of global reduction in protein synthesis. Along with the results obtained with the bicistronic gene reporter assays, our data support an IRES-like function of the 5'UTR *PTCH1b* mRNA.

Results obtained using MCF7 cells following the same experimental procedure were similar only in part (**Fig. S4**). The GLI1 expression vector led to an increase in total *PTCH1b* mRNA both in normoxia and in hypoxia. The hypoxic culture condition was better tolerated by MCF7 cells, based on the effect the treatment had on global protein synthesis. The majority of *PTCH1b* mRNA was polysome-associated in normoxia. GLI1 expression plasmid was associated with higher association of the *PTCH1b* mRNA with the polysomes in normoxia. Contrary to the results in HEK 293T cells, however, GLI1 overexpression was associated with a strong decrease in cytoplasmic *PTCH1b* mRNAs, although the relative translation efficiency estimated from the distribution of mRNA between polysomal and subpolysomal fractions appeared to be increased by hypoxia for *PTCH1b* and *c-MYC* but not *PCNA* mRNAs. We were however, unable to visualize the PTC1-L protein in MCF7 extracts. Examples of the polysome fractionation are presented in **Figure S5**.
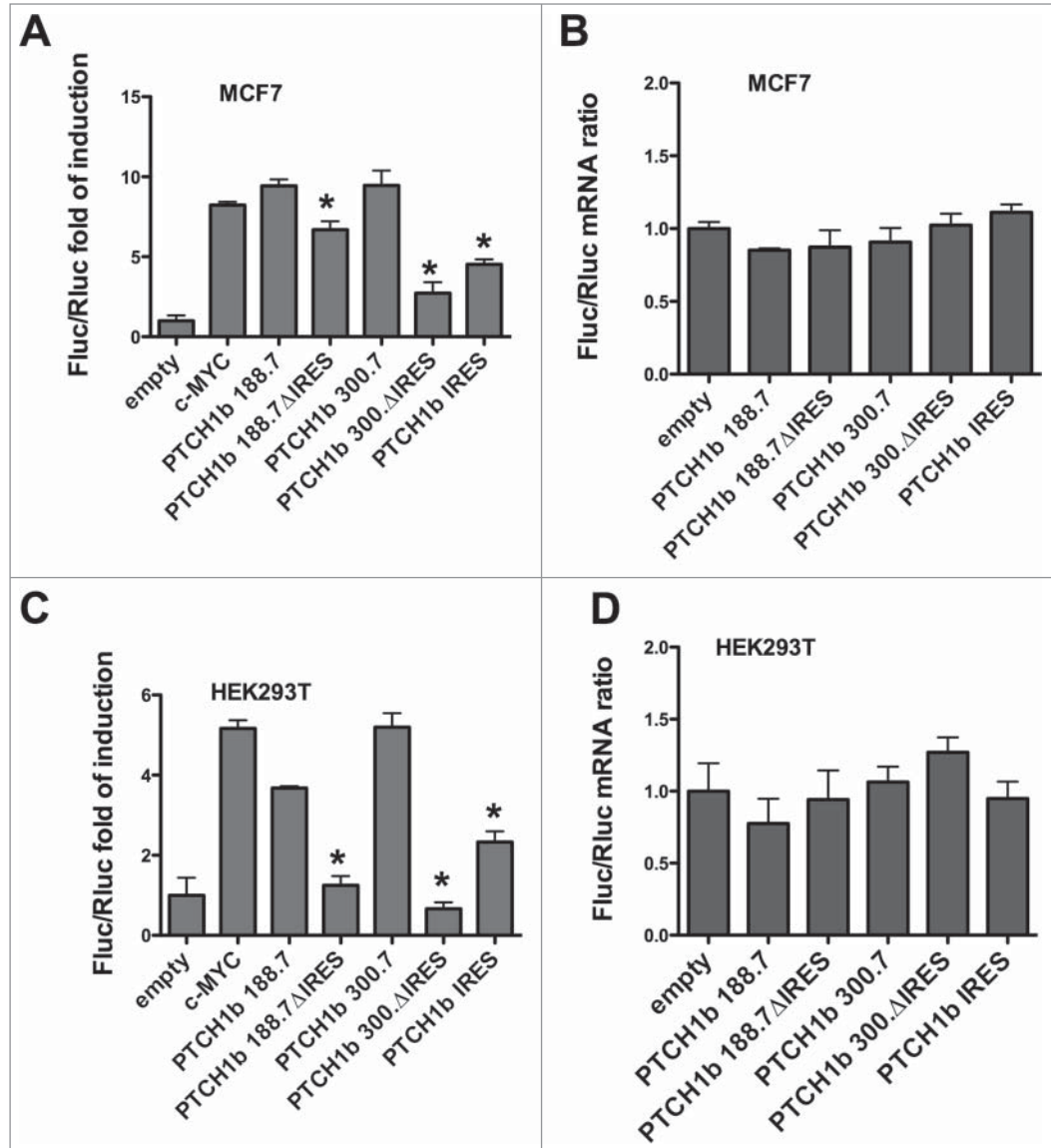
Figure 5. An internal ribosome entry site (IRES) motif maps in the 3′ end of the *PTCH1b* 5′UTR. (**A**) Putative *PTCH1b* IRES motif cloned into pRuF-type plasmid is not sufficient to obtain Firefly luciferase (Fluc) activity observed with the complete *PTCH1b* 5′UTR in MCF7 cells, while the remaining part of *PTCH1b* 5′UTRs (188ΔIRES and 300ΔIRES) retains certain levels of IRES activity. (**B**) Similar results were obtained in HEK 293T cells. (**C**) The ratios between Fluc and *Renilla* luciferase (Rluc) mRNA for remodeled pRuF *PTCH1b* 5′UTR plasmids in transfected MCF7 cells didn't deviate from 1.0. (**D**) The same results were obtained in HEK 293T cells. Results are presented as described in **Figure 4**.

Discussion

The *PTCH1* tumor suppressor gene encodes for a receptor with a negative regulatory role in the Hh-Gli signaling pathway. Constitutive activation of this pathway can be induced by the inactivation of *PTCH1* gene, which can be caused by means of different genetic and epigenetic mechanisms.[43–46] The fact that proper amount of PTC1 protein is needed for performing its tasks provides evidence that fine-tuned elements are a prerequisite to properly regulate the Hh-Gli signaling pathway.[47]

Even though much is known about the genomic organization of *PTCH1* gene, its transcripts and the protein products, much less is known about the transcriptional regulation of *PTCH1* transcripts, and even less is known about the role of 5′UTR in the regulation of their expression. In the 5′UTR of *PTCH1* transcript 1b a novel polymorphism involving a CGG trinucleotide repeat, separated from main AUG codon only by the
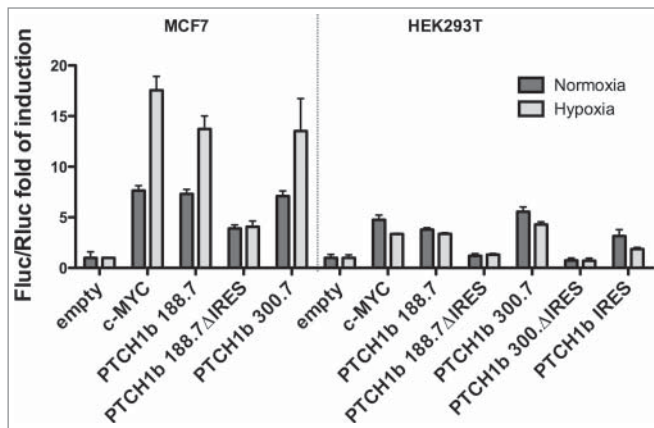
Figure 6. Hypoxia enhances *PTCH1b* 5'UTR mediated translation. MCF7 and HEK 293T cells transiently transfected with the different pRuF reporter constructs were grown in normoxic (dark gray) or severe hypoxic (light gray) conditions for 16 hours. Luciferase assays were performed as described in **Materials and Methods** and shown as those presented in **Figure 5**.

CAAC tetranucleotide, was discovered by Nagao et al.[32] The major allele contained 7 CGG repeats, while the minor allele contained 8 (rs71366293). In our previous research in patients with different types of ovarian neoplasms and healthy controls, we identified 2 additional alleles – $(CGG)_5$, which was found in one healthy control sample, and $(CGG)_6$ allele, which was found in one ovarian cancer patient.[35] Since the initial discovery of this trinucleotide repeat variant, its proximity to the AUG codon suggested that the number of CGG repeats could affect the efficacy of 5'UTR in its regulatory role of *PTCH1b* expression. To address this issue, 2 functional analyses have been published so far. A functional analysis was conducted by cloning various $(CGG)_n$CAAC constructs downstream of SV40 (Simian vacuolating virus 40) promoter and upstream of luciferase reporter gene (Fluc).[32] The results of luciferase assays, performed 24 h post-transfection in HEK 293T cells, revealed a positive correlation between the CGG-repeat number and the luciferase activity, although statistical analysis of the differences was not provided. Fluc mRNA quantification showed no differences in the reporter gene transcription levels regarding the CGG-repeat number, leading to the conclusion that the increase in luciferase activity with the expansion of CGG repeats is due to the increased efficiency of Firefly luciferase translation. The fact that the CGG-repeat polymorphism was taken out of the context of the complete *PTCH1b* 5'UTR is a potential limitation of that study, since the presence of different *cis*-regulatory elements that could drive *PTCH1b* expression regulation, and whose proper activity could be affected by the CGG-repeat polymorphism, could not be evaluated. In a recently published analysis, the complete 188nt-long *PTCH1b* 5'UTR sequence, harboring either 7 or 8 CGG repeats, was cloned into pGL4.10 vector downstream of TK (thymidine kinase) promoter and upstream of Fluc.[33] The results in HEK 293T cells showed dramatically reduced reporter activity for plasmid harboring 8 CGG repeats, with no effect on Fluc transcription compared

with the 7 CGGs construct. Consequently, both studies concluded that the CGG-repeat number could potentially alter the *PTCH1b* expression at translational level, which might have an effect on the severity of the disease in which certain CGG-repeat alleles were found.

In our study we wanted to re-evaluate a potential effect of CGG-repeat polymorphism, starting from alleles found in the Croatian population. Transcription and/or translation of downstream mRNA in a context of the complete *PTCH1b* 5'UTR sequence was studied, taking also into account that in 2 major nucleotide databases and literature, *PTCH1b* 5'UTR is annotated in 3 different lengths – 188, 300 and 372 nucleotides. Using different luciferase reporter constructs in assays with 3 established human cell lines – one non-cancerous (HEK 293T) and 2 derived from colon and breast carcinomas (HCT116 and MCF7) – our study showed that the number of CGG repeats has no significant impact on the activity of Firefly luciferase. The allele with 5 CGG repeats led to a slight, albeit statistically significant, increase in activity of the reporter gene, and this was obtained only in the context of 188nt-long 5'UTR. Computational prediction of *PTCH1b* 5'UTR secondary structure using *mfold* software indicated a slight increase in the stability of secondary structure with the increasing number of CGG repeats, which however could only have a moderate impact on the efficiency of the PTC1-L translation (data not shown).[48] Generally, we observed that insertion of *PTCH1b* 5'UTR into the pGL3-Promoter plasmid led to a significant increase in reporter gene transcription and this finding was in contrast with previous results. In our hands, it seems that the *PTCH1b* 5'UTR could have an enhancing effect on transcription. RegRNA 2.0 web-server predicted various transcriptional regulatory motifs, mostly located within the 188nt-long *PTCH1b* 5'UTR sequence.[49] The most abundant motifs are binding sites for BEN, ZF5 and ETF transcription factors, of which ETF has a consensus binding site "GCGGCGG".[50] Similarly, for 5'UTR of the fragile X mental retardation 1 gene (*FMR1*) it was found that CGG repeats enhances the transcription of *FMR1* by means of CGGBP-20 transcription factor, coded by the CGG triplet repeat binding protein 1 gene (*CGGBP1*).[51,52]

Taken all together, our results showed that the number of CGG repeats, in the context of the complete 5'UTR, could not have a significant impact on either mRNA or protein expression of *PTCH1b*. While only alleles with a relatively small number of CGG repeats have been found (3 and 5 to 8), so far no unambiguous association of a certain number of CGG repeats with disease has been demonstrated, as noted in Musani et al.[35] All these observations support the thesis that this *PTCH1* polymorphism could not be a genetic background (a causal mutation) of a trinucleotide repeat disorder-like disease.

On average, at least a 2-fold reduction in Firefly luciferase activity compared to the empty pGL3-Promoter backbone was observed for plasmids harboring longer, 300- or 372nt-long *PTCH1b* 5'UTR. One possible explanation for this finding could be that those longer and with high GC-content *PTCH1b* 5'UTRs form more stable secondary structures, which hinder the mRNA unwinding capacity of the translation initiation complex,
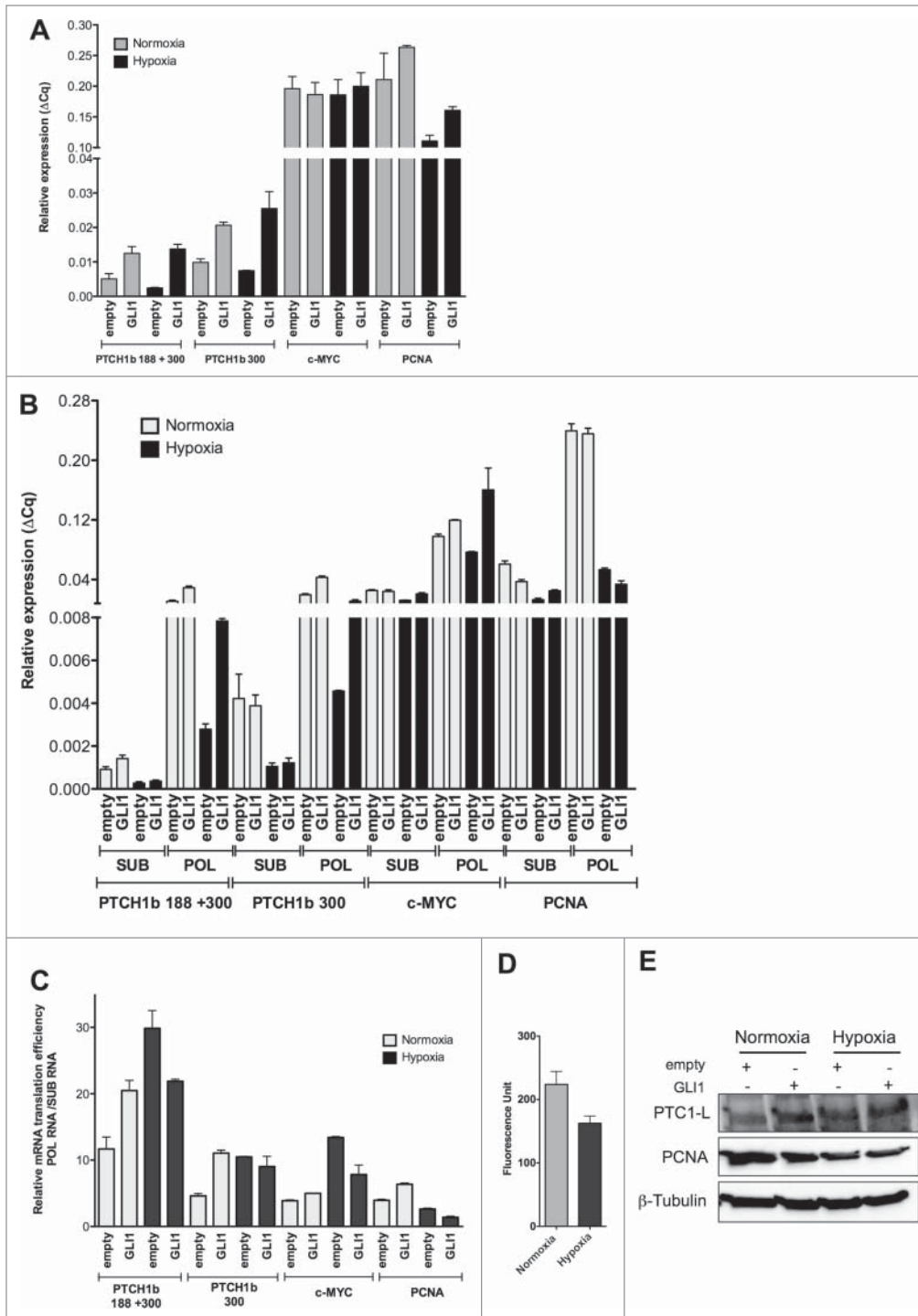
Figure 7. Higher *PTCH1b* mRNA relative translation efficiency during hypoxia in HEK 293T cells overexpressing GLI1. HEK 293T cells were transfected with an empty vector or a construct overexpressing GLI1 and then cultured in normoxia or hypoxia for 16 hours (48 hours post transfection). (**A**). Total RNA levels of the indicated mRNAs, quantified by qPCR as described in the method section and presented as relative expression compared to the reference genes (ΔCq). *c-MYC* mRNA was included as an example of mRNA whose 5'UTR is considered to possess IRES activity, while *PCNA* was included as negative control for IRES function. Error bars plot the average and standard deviations of 3 replicates (**B**). Cytoplasmic lysates of HEK 293T cells transfected and cultured as for panel A, were separated by sucrose-gradient equilibrium density; subpolysomal (SUB) and polysome-associated (POL) mRNAs were identified and collected by UVC scanning and the indicated transcripts were quantified by qPCR, as for panel **A**. (**C**). The results from panel B, are also plotted as ratio between polysome-associated and subpolysomal mRNAs as a function of the different treatment. This ratio is considered an estimate of relative mRNA translation efficiency. (**D**). Global relative mRNA translation rates in HEK 293T cells cultures in normoxia or hypoxia for 16 hours were assessed by incorporation of an immune-detectable methionine analog, as described in **Materials and Methods**. (**E**). Western blot analysis of PTC1-L protein and PCNA. Transfection of the GLI1 overexpression plasmid and treatment are indicated. Beta-tubulin was used as reference protein.

thus lowering the efficiency of protein synthesis.[53] However, when the longest *PTCH1b* 5'UTR sequence was computationally analyzed, there was a prediction of 2 potential upstream open reading frames (uORFs) and, more significantly, one upstream AUG codon present only within the 300- or 372nt-long *PTCH1b* 5'UTRs (Fig. 2A). After removing 2 out of 3 uAUG codons, of which one was predicted to create an overlapping open reading frame that could potentially interfere with translation from the canonical *PTCH1b* ORF and thus reduce the PTC1-L levels, luciferase activity was restored to the level observed with the 188nt-long *PTCH1b* 5'UTR.[54] The introduced mutations did not affect the levels of Fluc mRNA, indicating that the observed difference in luciferase activity must be ascribed to post-transcriptional control.

Quantification of *PTCH1b* mRNA targeting either transcripts containing 5'UTR of at least a 188nt length or of those containing at least a 300nt-long 5'UTR, allowed us to estimate that transcript(s) with long UTR(s) is highly prevalent in standard culture conditions in HCT116 ^P53+/+ and MCF7 cells while the ratio is less skewed after induction of *PTCH1b* by GLI1 overexpression. The preference for longer *PTCH1b* transcripts could be one form of spatio-temporal regulation of translation, utilized when lower and more tightly regulated levels of PTC1-L are needed.[55]

Characteristics and presence of different *cis*-regulatory elements led us to hypothesize that *PTCH1b* 5'UTR in general affect the efficiency of cap-dependent initiation of PTC1-L translation.[56] This might even anticipate that *PTCH1b* 5'UTR possesses a capability to initiate cap-independent, an internal ribosome entry site-driven translation of PTC1-L.[57,58] Although the number of reports on cellular IRESes is increasing, their existence still raises skepticism and is often subject of scientific debates, mainly due to concerns about the lack of unambiguous experimental verifications.[59,60] The fact that there are a growing number of cancer-related genes whose translation regulation can be subjected to cap-independent initiation makes the quest for discovering and testing new putative cellular IRESes even more meaningful.[61] The results of luciferase assays with bicistronic plasmids proved our assumptions showing that both 188- and 300nt-long 5'UTRs significantly increased the activity of downstream reporter gene, but with no differences among the repeat numbers. The increased Fluc activity was proven not to be due to either a potential cryptic promoter activity of *PTCH1b* 5'UTR or an alternative splicing event. Thus, we were able to conclude that observed higher Fluc activity, with equal amount of both Rluc and Fluc mRNA should be a post-transcriptional, namely a translational effect. When the first 76 bp nucleotides from the 3' portion of *PTCH1b* 5'UTR, which were predicted to bear a cellular internal ribosome entry site, were removed from either 188- or 300nt-long pRuF-type plasmid, the Fluc luciferase activity was significantly, albeit not completely, reduced. At the same time, those 76 nucleotides alone were not sufficient to obtain the complete IRES activity of intact 5'UTRs. This could indicate that the putative IRES motif spans over a larger part of the *PTCH1b* 5'UTR, potentially even extending to the coding region, or that contiguous part(s) of *PTCH1b* 5'UTR harbor binding sites for IRES *trans*-acting factors (ITAFs), required for

proper folding and function of the IRES motif itself.[62] The results achieved with remodeled pRuF-based *PTCH1b* 5'UTR plasmids were also proven to be due to the translational and not transcriptional processes. Considering all these results, our study has presented strong evidences that *PTCH1b* 5'UTR contains an internal ribosome entry site, and is thus potentially capable to initiate PTC1-L translation in cap-independent manner. According to the IRESite database, although there aren't similarities with known virus IRES motifs, there are a few eukaryotic genes whose 5'UTR contains proven cellular IRES and shares a similarity with the sequence of putative *PTCH1b* IRES motif.[63] More interestingly, the highest similarity lies in the presence of CGG-repeat element. Such genes, having at least 3 CGG repeats within their IRES motifs, include previously mentioned *FMR1* gene, jun proto-oncogene (*JUN*), ornithine decarboxylase 1 (*ODC1*), B-cell CLL/lymphoma 2 (*BCL2*), and BCL2-associated athanogene (*BAG1*).[64–68]

Since it was discovered that hypoxic conditions activate the Hh-Gli pathway, and it is already known that several genes are being translated under the hypoxia by IRES-dependent mechanism, we wanted to explore if the putative *PTCH1b* 5'UTR IRES can be activated by oxygen deprivation condition.[42,69] The increased activity of putative IRES element within the 5'UTR of *PTCH1b* has been observed in transfected MCF7 cells after exposure to strong hypoxic conditions, while in HEK 293T hypoxia did not increase, in fact decreased, the activity of *PTCH1b* IRES element. The presence of an IRES element within *PTCH1b* 5'UTR could thus allow PTC1-L to be synthesized in conditions when the general level of cellular protein synthesis is reduced, such as under low oxygen levels, what is also important in tumor development and metastasis, or for the potential therapeutic role of activated Hh-Gli pathway in acute or chronic ischemic heart disease.[70,71] To further explore this possibility, we conducted polysomal profiling using HEK 293T cells cultured in normoxia or hypoxia, transfected or not with a GLI1 overexpression plasmid and we quantified the relative association of *PTCH1b* transcripts with the polysomes as well as the changes in expression at the level of total RNA. Levels of PTC1-L protein were also measured by Western blot. Results support higher relative translation efficiency of *PTCH1b* mRNA in condition of reduced global protein synthesis, particularly upon GLI1 ectopic expression (**Fig. 7, S4 and S5**).

The activation of the IRES motif could also allow to overcome the negative effect of uORFs and uAUG within the 300- or 372nt-long 5'UTR transcripts. Coupled to our observation that GLI1 overexpression can induce the transcription of *PTCH1b* transcripts containing both the short and the longer 5'UTR, these results could lead to hypothesize that the ensuing negative feedback loop can also be fine-tuned at post-transcriptional level by the competition between uAUG/uORF translation inhibition and IRES-dependent translation initiation. In conclusion, all these results point to the exceptionally complex and so far unexplored levels of *PTCH1b* expression regulation by 5'UTR, each of which needs further mechanistic explanations. So far, we can assert that *PTCH1b* 5'UTR shares its characteristics with mRNAs coding for transcription factors, proto-oncogenes,

growth factors and their receptors, or generally for proteins poorly translated under normal conditions.[72]

Materials and Methods

Plasmid construction

As DNA template for the amplification of human *PTCH1b* 5'UTRs of different length we used genomic DNA obtained from our previous studies.[35,73] For the alleles harboring 5, 7 and 8 CGG repeats we used genomic DNA from healthy control samples having $(CGG)_5/(CGG)_7$, $(CGG)_7/(CGG)_7$ and $(CGG)_8/(CGG)_8$ genotypes, respectively. For the allele with 6 CGG repeats we used a genomic DNA sample collected from an ovarian cancer patient with the $(CGG)_6/(CGG)_8$ heterozygous genotype. Due to high GC-content in the proximity of the CGG repeats, the complete *PTCH1b* 5'UTR (either 188-, 300- or 372-nucleotide long) plus the first 21 coding nucleotides of *PTCH1b* sequence was amplified using nested PCR approach in which inner forward primers contained restriction sites for HindIII-XbaI-EcoRI enzymes at their 5' end, while only one inner reverse primer with NcoI site was used (all primers' sequences and PCR conditions used for plasmid construction are available upon request). The amplicons were cloned using HindIII and NcoI restriction enzymes into the commercial pGL3-Promoter vector (Promega, Milan, Italy) immediately upstream and in-frame with the Firefly cDNA start codon and just downstream of the SV40-derived promoter.

ATGpr and NetStart 1.0 tools were used for predicting potential upstream open reading frames.[36,37] Two out of 3 upstream translation initiation codons, namely uAUG2 and uAUG3 (Fig. 2A), were mutated in the pGL3-P PTCH1 300.7 plasmid using GENEART Site-Directed Mutagenesis System (Invitrogen, Milan, Italy) according to the manufacturer's instructions. Two complementary mutagenic oligonucleotide primers each harboring 2 nucleotide changes (F_SDM 5'- ACCCCCGCGCAAT**T**-TGGCA**T**TGGAAGGCGCAGGGTCTGAC-3' and R_SDM 5'- GTCAGACCCTGCGCCTTCCA**A**TGCCA**A**ATTGCGC-GGGGGT-3', variant nucleotides are in bold) created pGL3-P PTCH1 300/7 SDM plasmid with AU**G**>AU**U** and **A**UG>**U**UG mutations, respectively.

For the construction of pRuF bicistronic vectors, the complete 188- or 300-nucleotide long *PTCH1b* 5'UTR containing either 5, 7 or 8 CGG repeat plus first 21 nucleotides of *PTCH1b* coding sequence was amplified using the previously described nested PCR approach and the same inner forward primers, while the inner reverse primer used contained the restriction site for the XhoI enzyme. The amplicons were cloned using EcoRI and XhoI endonucleases into the pRuF-empty backbone, as the intervening sequence between *Renilla* and Firefly luciferase genes. The construction of pRuF-empty vector backbone was previously published.[34] The rationale behind this approach is that transcription driven from an upstream promoter (in our case SV40) should give origin to one bicistronic mRNA transcript, from which the translation of the upstream reporter (*Renilla* luciferase) should occur through the cap-

dependent mechanism, whereas the downstream reporter (Firefly luciferase) should be translated only if the inserted sequence exhibits IRES activity, thus allowing ribosomes to be recruited to the mRNA internally.[74] The same dual reporter vector without inserted fragment (empty) was used as a negative control, while as a positive control we used pRuF plasmid with cloned c-MYC 5'UTR region which contains a previously identified IRES site.[39] Since the UTRscan tool predicts that the first 76 nucleotides at the 3' end of *PTCH1b* 5'UTR (c.-76_-1 for the allele with 7 CGG repeats) harbors a putative IRES, we built 3 additional pRuF constructs with the aim to map the putative IRES sequence.[75] We used double stranded linkers with cohesive ends that are complementary to ends generated after endonuclease digestion of the plasmid containing the full length 5'UTR sequence to obtain pRuF plasmids containing just the 76nt predicted IRES or lacking that region from either the 188nt ot 300nt sequence. The procedure is described in **Supplemental Methods** and depicted in **Supplemental Figure S2**.

DH5α competent cells were used for plasmid propagation and all plasmid clones were checked by restriction mapping and direct DNA sequencing (BMR Genomics, Padua, Italy). Transfection grade plasmids were obtained using the Pure Yield Midiprep system according to the manufacturer's instructions (Promega, Milan, Italy).

Cell lines, culture conditions and treatment procedure

Human breast adenocarcinoma-derived MCF7 and Human Embryonic Kidney HEK 293T cells were obtained from the InterLab Cell Line Collection (ICLC, Azienda Ospedaliera Universitaria San Martino-IST, Genoa, Italy). Human colon cancer cells expressing wild type p53, HCT116 $^{p53+/+}$ were obtained from the Vogelstein lab (The Johns Hopkins Kimmel Cancer Center, Baltimore, USA). Cells were maintained in either DMEM or RPMI medium supplemented with 10% Fetal Bovine Serum (FCS), 2mM L-Glutamine and antibiotics (100 units/ml penicillin plus 100 mg/ml streptomycin) in humidified atmosphere at 37°C and 5% CO_2. Cells were routinely checked to exclude the presence of mycoplasma. For hypoxic conditions, MCF7 and HEK 293T cells were cultured for 16 hours in the GENbox plastic jar with the GENbag hypoxia generator (Biomerieux, Florence, Italy).

Dual-Luciferase Reporter Assays

Cells for luciferase assays were seeded in 24-well plates 24 h before transfection. Cells were transfected at 50-70% confluence using Myrus LT-1 transfection reagent (Tema Ricerca, Milan, Italy), according to the manufacturer's instructions. Specifically, 350 ng of pGL3-Promoter-based vectors were used along with 50 ng of the control pRL-SV40 plasmid, introduced to normalize the transfection efficiency. In assays where pRuF-type plasmids were tested, 400 ng of plasmid DNA was transfected. Cells were harvested 24 h after transfection and luciferase assays were carried out using the dual-luciferase assay (Promega, Milan, Italy) as previously described.[34] Briefly, 24 h after transfection cells where lysed with Passive Lysis Buffer (PLB) 1X and both Firefly

and *Renilla* luciferase activity was measured with the Infinite M200 multi-plate reader (Tecan, Milan, Italy). In the experiments that needed IRES activation, 8 hours after transfection cells were cultured in hypoxia conditions for additional 16 hours prior to the luciferase assay. Results are presented as the average relative light units and the standard deviations of at least 3 independent biological repeats.

Genomic DNA/total RNA extraction and qPCR quantification

Cells were seeded into 6-well plates and transfected at 50–70% confluence with 1.2 μg of either pGL-P- or pRuF-type reporter vectors using Myrus LT-1 transfection reagent (Tema Ricerca, Milan, Italy). To endogenously activate the Hedgehog-Gli pathway, cells were transfected with 2 μg/well of pcDNA4nlSMtGLI1 plasmid, while pCMV-NEO-BAM plasmid DNA was used as a negative control. pcDNA4nlSMtGLI1 (kind gift from Prof. Fritz Aberger) is an expression vector for the GLI1 transcription factor, the main transcriptional activator of Hh-Gli target genes.[76]

Twenty-four hours after transfection with luciferase reporter vectors, or 48 h after transfection with pcDNA4nlSMtGLI1/pCMV-NEO-BAM plasmid, cells were harvested and washed once with phosphate buffer saline (PBS). Total RNA was extracted from the cells transfected with either pRuF-type or pcDNA4nlSMtGLI1/pCMV-NEO-BAM plasmids using the RNAeasy mini Kit (Qiagen, Milan, Italy) according to the manufacturer's instructions. From the cells transfected with pGL-P-based plasmids, both total RNA and genomic DNA were extracted using AllPrep DNA/RNA Mini Kit (Qiagen, Milan, Italy). In-column DNAse treatment (Qiagen, Milan, Italy) was always performed to remove DNA contamination during total RNA extraction. DNA or RNA purity and concentration were evaluated using the NanoDrop ND1000 spectrophotometer.

cDNA was generated starting from 1 μg of total RNA by using the RevertAidTM First Strand cDNA Synthesis Kit (ThermoFisher, Milan, Italy). Quantitative Real-time PCR was performed using a cDNA aliquot equivalent to 25 ng of converted RNA or with 10 ng of gDNA using either CFX96 or CFX386 Real-Time PCR Detection System (BioRad, Milan, Italy) and the 2X KAPA SYBRGreen FAST qPCR Master Mix (Kapa Biosystems, Resnova, Ancona, Italy). The relative quantitation of various endogenous mRNAs was calculated using the comparative Ct method ($\Delta\Delta$Ct), taking into account the efficiency of cDNA synthesis by the quantification of the glyceraldehyde-3-phosphate dehydrogenase (GAPDH) and β-2-microglobulin (B2M) reference genes, as previously described.[34]

In the cells transfected with the monocistronic pGL3-P-based plasmids we quantified the Firefly luciferase (Fluc) mRNA using specific primers (Eurofins MWG Operon, Ebersberg, Germany – all primers' sequences used for qPCR are available upon request). To take into account differences in transfection efficiencies, we also quantified that specific Fluc fragment in the plasmid DNA-containing gDNA extracts, thus obtaining the average plasmid copy number. From the cells transfected with bicistronic dual-luciferase pRuF-based plasmids we quantified the mRNA of both Fluc and Rluc gene. Since *PTCH1b* 5'UTR is officially annotated in 2 different sizes, and a third even longer one was reported, we wanted to inspect if *PTCH1b* transcripts containing different 5'UTRs are equally expressed under basal level of Hh-Gli activity or after ectopic GLI1 overexpression, a condition used to mimic the activated state of the pathway. We quantified separately the expression of *PTCH1b* transcripts containing a 5'UTR of at least 188nt length or of at least 300nt. To this aim a common reverse primer spanning the exon 1/exon 2 boundary (5'-ATTTC-CAAGGGGAAGGCTACTGGCC-3') was used and paired with specific forward primers positioned at the very beginning of the 188nt (5'-GCGCCCGCCGTGTGAGCAGCAGCAG-3') or 300nt (5'-GAACTGGATGTGGGCAGCGGCGGCC-3') 5'UTR. As the forward primer for the shorter variant of the UTR could not be selective, but can amplify from the 300nt (or longer) UTR template, the actual relative changes in expression can be estimated by comparing the results of the 2 PCR reactions, after verifying comparable efficiency of both amplicons' synthesis.

Sucrose gradient fractionation of cytoplasmic cell lysates and polysomal profiling

Cytoplasmic lysates were prepared and fractionated using 10%–50% sucrose-gradients in ultracentrifuge tubes as previously described.[34,77] RNA associated with 2 or more ribosomes, labeled as POL fraction, were collected and analyzed separately from RNA co-sedimenting with individual ribosomal subunits or with the 80S, labeled as SUB fraction. Fractions were monitored for RNA content recovered after ultracentrifugation using UVC scanning with a Teledyne Isco system (Isco, Inc.., Lincoln, Nebraska, USA). RNA was recovered by organic solvent extraction and salt/ethanol precipitation and processed for qPCR analysis, following the protocol previously described.[34,77] The expression of the *PTCH1b* transcripts containing a 5'UTR of at least 188nt length or of at least 300nt were quantified using the primers described in the previous section.

High-content imaging analysis of global protein translation

To investigate the impact that hypoxia has on the global rate of protein synthesis, HEK 293T or MCF7 cells were cultured in normoxia or in the hypoxic chamber for a total of 16 hours. Three hours before analysis, the culture medium was removed and replaced with fresh, methionine-free medium supplemented with an methionine analog, following the procedure of the Click-iT→ HPG Alexa Fluor→ 488 Protein Synthesis Assay Kit (Molecular Probes, Invitrogen, Life Technologies). Relative quantification of protein synthesis was performed by acquiring images by the PerkinElmer Operetta→ High Content Imaging System, using DAPI staining to visualize nuclei. Images were analyzed and quantified by Columbus software.

Western Blot analysis

Soluble proteins from HEK 293T cells were extracted using RIPA lysis buffer supplemented with Protease Inhibitor cocktail (Roche, Milan, Italy). Protein extracts were quantified using the

BCA Protein Assay kit following the manufacturer's recommendations (Thermo, Milan, Italy) and 100 μg were loaded into 12% PolyAcrylamide gels. SDS-PAGE was performed as previously described using the following antibodies: PTC1-L (patched, G-19 sc-6149 from Santa Cruz), PCNA (F-2, Santa Cruz), β-tubulin (3F3-G2, Santa Cruz) and the ECL select reagent (Amersham, GE-Health Care, Milan, Italy) with a ChemiDoc XRS+ documentation system with ImageLab software (BioRad, Milan, Italy).[77]

Statistical analysis

Differences in luciferase activity and mRNA expression between various plasmids were analyzed by one-way analysis of variance (ANOVA), followed by Tukey's post-hoc test for multiple comparisons. Expression of differently sized *PTCH1b* 5'UTRs under basal level and endogenously activated Hh-Gli pathway, and the effect of hypoxia on the activity of pRuF-type plasmids were analyzed by regular 2-way ANOVA, followed by Tukey's post-hoc test. Two-tailed *P*-values less than 0.05 were considered statistically significant. Statistical analyses were performed using Prism 6 for Windows software, version 6.04 (GraphPad Software, USA).

Supplemental Material

Supplemental data for this article can be accessed on the publisher's website.

References

1 Briscoe J, Thérond PP. The mechanisms of Hedgehog signaling and its roles in development and disease. Nat Rev Mol Cell Biol 2013; 14:416–29; PMID:23719536; http://dx.doi.org/10.1038/nrm3598

2 Nieuwenhuis E, Hui C. Hedgehog signaling and congenital malformations. Clin Genet 2005; 67:193–208; PMID:15691355; http://dx.doi.org/10.1111/j.1399-0004.2004.00360.x

3 Kiesslich T, Neureiter D. Advances in targeting the Hedgehog signaling pathway in cancer therapy. Expert Opin Ther Targets 2012; 16:151–6; PMID:22233124; http://dx.doi.org/10.1517/14728222.2012.652948

4 Bürglin TR. The Hedgehog protein family. Genome Biol 2008; 9:241; PMID:19040769; http://dx.doi.org/10.1186/gb-2008-9-11-241

5 Marigo V, Davey RA, Zuo Y, Cunningham JM, Tabin CJ. Biochemical evidence that patched is the Hedgehog receptor. Nature 1996; 384:176–9; PMID:8906794; http://dx.doi.org/10.1038/384176a0

6 Ayers KL, Thérond PP. Evaluating Smoothened as a G-protein-coupled receptor for Hedgehog signalling. Trends Cell Biol 2010; 20:287–98; PMID:20207148; http://dx.doi.org/10.1016/j.tcb.2010.02.002

7 Wilson CW, Stainier DYR. Vertebrate Hedgehog signaling: cilia rule. BMC Biol 2010; 8:102; PMID:20687907; http://dx.doi.org/10.1186/1741-7007-8-102

8 Lipinski RJ, Gipp JJ, Zhang J, Doles JD, Bushman W. Unique and complimentary activities of the Gli transcription factors in Hedgehog signaling. Exp Cell Res 2006; 312:1925–38; PMID:16571352; http://dx.doi.org/10.1016/j.yexcr.2006.02.019

9 Katoh Y, Katoh M. Hedgehog target genes: mechanisms of carcinogenesis induced by aberrant hedgehog signaling activation. Curr Mol Med 2009; 9:873–86; PMID:19860666; http://dx.doi.org/10.2174/156652409789105570

10 McMahon AP, Ingham PW, Tabin CJ. Developmental roles and clinical significance of hedgehog signaling. Curr Top Dev Biol 2003; 53:1–114; PMID:12509125; http://dx.doi.org/10.1016/S0070-2153(03)53002-2

11 Lai K, Robertson MJ, Schaffer D V. The sonic hedgehog signaling system as a bistable genetic switch. Biophys J 2004; 86:2748–57; PMID:15111393; http://dx.doi.org/10.1016/S0006-3495(04)74328-3

12 Bak M, Hansen C, Friis Henriksen K, Tommerup N. The human hedgehog-interacting protein gene: structure and chromosome mapping to 4q31.21->q31.3. Cytogenet Cell Genet 2001; 92:300–3; PMID:11435703; http://dx.doi.org/10.1159/000056918

13 Ribes V, Briscoe J. Establishing and interpreting graded Sonic Hedgehog signaling during vertebrate neural tube patterning: the role of negative feedback. Cold Spring Harb Perspect Biol 2009; 1:a002014; PMID:20066087; http://dx.doi.org/10.1101/cshperspect.a002014

14 Hahn H, Christiansen J, Wicking C, Zaphiropoulos PG, Chidambaram A, Gerrard B, Vorechovsky I, Bale AE, Toftgard R, Dean M, et al. A mammalian patched homolog is expressed in target tissues of sonic hedgehog and maps to a region associated with developmental abnormalities. J Biol Chem 1996; 271:12125–8; PMID:8647801; http://dx.doi.org/10.1074/jbc.271.21.12125

15 Kogerman P, Krause D, Rahnama F, Kogerman L, Undén AB, Zaphiropoulos PG, Toftgård R. Alternative first exons of PTCH1 are differentially regulated in vivo and may confer different functions to the PTCH1 protein. Oncogene 2002; 21:6007–16; PMID:12203113; http://dx.doi.org/10.1038/sj.onc.1205865

16 Shimokawa T, Rahnama F, Zaphiropoulos PG. A novel first exon of the Patched1 gene is upregulated by Hedgehog signaling resulting in a protein with pathway inhibitory functions. FEBS Lett 2004; 578:157–62; PMID:15581634; http://dx.doi.org/10.1016/j.febslet.2004.11.006

17 Shimokawa T, Svärd J, Heby-Henricson K, Teglund S, Toftgård R, Zaphiropoulos PG. Distinct roles of first exon variants of the tumor-suppressor Patched1 in Hedgehog signaling. Oncogene 2007; 26:4889–96; PMID:17310997; http://dx.doi.org/10.1038/sj.onc.1210301

18 Nagao K, Toyoda M, Takeuchi-Inoue K, Fujii K, Yamada M, Miyashita T. Identification and characterization of multiple isoforms of a murine and human tumor suppressor, patched, having distinct first exons. Genomics 2005; 85:462–71; PMID:15780749; http://dx.doi.org/10.1016/j.ygeno.2004.11.014

19 Suzuki M, Hatsuse H, Nagao K, Takayama Y, Kameyama K, Kabasawa Y, Omura K, Yoshida M, Fujii K, Miyashita T. Selective haploinsufficiency of longer isoforms of PTCH1 protein can cause nevoid basal cell carcinoma syndrome. J Hum Genet 2012; 57:422–6; PMID:22572734; http://dx.doi.org/10.1038/jhg.2012.45

20 Agren M, Kogerman P, Kleman MI, Wessling M, Toftgård R. Expression of the PTCH1 tumor suppressor gene is regulated by alternative promoters and a single functional Gli-binding site. Gene 2004; 330:101–14; PMID:15087129; http://dx.doi.org/10.1016/j.gene.2004.01.010

21 Levanat S, Gorlin RJ, Fallet S, Johnson DR, Fantasia JE, Bale AE. A two-hit model for developmental defects in Gorlin syndrome. Nat Genet 1996; 12:85–7; PMID:8528259; http://dx.doi.org/10.1038/ng0196-85

22 Hahn H, Wicking C, Zaphiropoulous PG, Gailani MR, Shanley S, Chidambaram A, Vorechovsky I, Holmberg E, Unden AB, Gillies S, et al. Mutations of the human homolog of Drosophila patched in the nevoid basal cell carcinoma syndrome. Cell 1996; 85:841–51; PMID:8681379; http://dx.doi.org/10.1016/S0092-8674(00)81268-4

23 Kimonis VE, Goldstein AM, Pastakia B, Yang ML, Kase R, DiGiovanna JJ, Bale AE, Bale SJ. Clinical manifestations in 105 persons with nevoid basal cell carcinoma syndrome. Am J Med Genet 1997; 69:299–308; PMID:9096761; http://dx.doi.org/10.1002/(SICI)1096-8628(19970331)69:3%3c299::AID-AJMG16%3e3.0.CO;2-M

24 Pan S, Dong Q, Sun L-S, Li T-J. Mechanisms of inactivation of PTCH1 gene in nevoid basal cell carcinoma syndrome: modification of the two-hit hypothesis. Clin Cancer Res 2010; 16:442–50; PMID:20068110; http://dx.doi.org/10.1158/1078-0432.CCR-09-2574

25 Van der Velden AW, Thomas AA. The role of the 5' untranslated region of an mRNA in translation regulation during development. Int J Biochem Cell Biol 1999; 31:87–106; PMID:10216946; http://dx.doi.org/10.1016/S1357-2725(98)00134-4

26 Chamas F, Sabban EL. Role of the 5' untranslated region (UTR) in the tissue-specific regulation of rat tryptophan hydroxylase gene expression by stress. J Neurochem 2002; 82:645–54; PMID:12153488; http://dx.doi.org/10.1046/j.1471-4159.2002.00989.x

27 Pickering BM, Willis AE. The implications of structured 5' untranslated regions on translation and disease. Semin Cell Dev Biol 2005; 16:39–47; PMID:15659338; http://dx.doi.org/10.1016/j.semcdb.2004.11.006

28 Araujo PR, Yoon K, Ko D, Smith AD, Qiao M, Suresh U, Burns SC, Penalva LOF. Before It Gets Started: Regulating Translation at the 5' UTR. Comp Funct Genomics 2012; 2012:475731; PMID:22693426; http://dx.doi.org/10.1155/2012/475731

29 Barrett LW, Fletcher S, Wilton SD. Regulation of eukaryotic gene expression by the untranslated gene regions and other non-coding elements. Cell Mol Life

Sci 2012; 69:3613–34; PMID:22538991; http://dx.doi.org/10.1007/s00018-012-0990-9

30 Maier T, Güell M, Serrano L. Correlation of mRNA and protein in complex biological samples. FEBS Lett 2009; 583:3966–73; PMID:19850042; http://dx.doi.org/10.1016/j.febslet.2009.10.036

31 Chatterjee S, Pal JK. Role of 5'- and 3'-untranslated regions of mRNAs in human diseases. Biol Cell 2009; 101:251–62; PMID:19275763; http://dx.doi.org/10.1042/BC20080104

32 Nagao K, Fujii K, Yamada M, Miyashita T. Identification of a novel polymorphism involving a CGG repeat in the PTCH gene and a genome-wide screening of CGG-containing genes. J Hum Genet 2004; 49:97–101; PMID:14735326; http://dx.doi.org/10.1007/s10038-003-0117-0

33 Tietze JK, Pfob M, Eggert M, von Preuβen A, Mehraein Y, Ruzicka T, Herzinger T. A non-coding mutation in the 5' untranslated region of patched homologue 1 predisposes to basal cell carcinoma. Exp Dermatol 2013; 22:834–5; PMID:24131384; http://dx.doi.org/10.1111/exd.12267

34 Bisio A, Nasti S, Jordan JJ, Gargiulo S, Pastorino L, Provenzani A, Quattrone A, Queirolo P, Bianchi-Scarrà G, Ghiorzo P, et al. Functional analysis of CDKN2A/p16INK4a 5'-UTR variants predisposing to melanoma. Hum Mol Genet 2010; 19:1479–91; PMID:20093296; http://dx.doi.org/10.1093/hmg/ddq022

35 Musani V, Sabol M, Car D, Ozretić P, Kalafatić D, Maurac I, Orešković S, Levanat S. PTCH1 gene polymorphisms in ovarian tumors: potential protective role of c.3944T allele. Gene 2013; 517:55–9; PMID:23313819; http://dx.doi.org/10.1016/j.gene.2012.12.089

36 Salamov AA, Nishikawa T, Swindells MB. Assessing protein coding region integrity in cDNA sequencing projects. Bioinformatics 1998; 14:384–90; PMID:9682051; http://dx.doi.org/10.1093/bioinformatics/14.5.384

37 Pedersen AG, Nielsen H. Neural network prediction of translation initiation sites in eukaryotes: perspectives for EST and genome analysis. Proc Int Conf Intell Syst Mol Biol 1997; 5:226–33; PMID:9322041

38 McGinnis S, Madden TL. BLAST: at the core of a powerful and diverse set of sequence analysis tools. Nucleic Acids Res 2004; 32:W20–5; PMID:15215342; http://dx.doi.org/10.1093/nar/gkh435

39 Stoneley M, Paulin FE, Le Quesne JP, Chappell SA, Willis AE. C-Myc 5' untranslated region contains an internal ribosome entry segment. Oncogene 1998; 16:423–8; PMID:9467968; http://dx.doi.org/10.1038/sj.onc.1201763

40 Le SY, Maizel J V. A common RNA structural motif involved in the internal initiation of translation of cellular mRNAs. Nucleic Acids Res 1997; 25:362–9; PMID:9016566; http://dx.doi.org/10.1093/nar/25.2.362

41 Spriggs KA, Bushell M, Willis AE. Translational regulation of gene expression during conditions of cell stress. Mol Cell 2010; 40:228–37; PMID:20965418; http://dx.doi.org/10.1016/j.molcel.2010.09.028

42 Bijlsma MF, Groot AP, Oduro JP, Franken RJ, Schoenmakers SHHF, Peppelenbosch MP, Spek CA. Hypoxia induces a hedgehog response mediated by HIF-1alpha. J Cell Mol Med 2009; 13:2053–60; PMID:18774959; http://dx.doi.org/10.1111/j.1582-4934.2008.00491.x

43 Musani V, Cretnik M, Situm M, Basta-Juzbasic A, Levanat S. Gorlin syndrome patient with large deletion in 9q22.32-q22.33 detected by quantitative multiplex fluorescent PCR. Dermatology 2009; 219:111–8; PMID:19439922; http://dx.doi.org/10.1159/000219247

44 Musani V, Sabol M, Car D, Ozretic P, Oreskovic S, Leovic D, Levanat S. LOH of PTCH1 region in BCC and ovarian carcinoma: microsatellite vs. HRM analysis. Front Biosci (Elite Ed) 2012; 4:1049–57; PMID:22201935; http://dx.doi.org/10.2741/E440

45 Cretnik M, Musani V, Oreskovic S, Leovic D, Levanat S. The Patched gene is epigenetically regulated in

ovarian dermoids and fibromas, but not in basocellular carcinomas. Int J Mol Med 2007; 19:875–83; PMID:17487419

46 Car D, Sabol M, Musani V, Ozretić P, Levanat S. Epigenetic regulation of the hedgehog-gli signaling pathway in cancer. Period Biol 2010; 112:419–23

47 Fodde R, Smits R. Cancer biology. A matter of dosage. Science 2002; 298:761–3; PMID:12399571; http://dx.doi.org/10.1126/science.1077707

48 Zuker M. Mfold web server for nucleic acid folding and hybridization prediction. Nucleic Acids Res 2003; 31:3406–15; PMID:12824337; http://dx.doi.org/10.1093/nar/gkg595

49 Chang T-H, Huang H-Y, Hsu JB-K, Weng S-L, Horng J-T, Huang H-D. An enhanced computational platform for investigating the roles of regulatory RNA and for identifying functional RNA motifs. BMC Bioinformatics 2013; 14(Suppl 2):S4; PMID:23369107

50 Kageyama R, Merlino GT, Pastan I. Nuclear factor ETF specifically stimulates transcription from promoters without a TATA box. J Biol Chem 1989; 264:15508–14; PMID:2768275

51 Chen L-S, Tassone F, Sahota P, Hagerman PJ. The (CGG)n repeat element within the 5' untranslated region of the FMR1 message provides both positive and negative cis effects on in vivo translation of a downstream reporter. Hum Mol Genet 2003; 12:3067–74; PMID:14519687; http://dx.doi.org/10.1093/hmg/ddg331

52 Gulyy PV, Orlov SV, Dizhe EB, Kuteikin-Teplyakov KB, Ignatovich IA, Zhuk SV, Perevozchikov AP. Roles of ZF5 and CGGBP-20 transcription factors in regulating expression of human FMR1 gene responsible for fragile X-syndrome. Cell tissue biol 2010; 4:54–62; PMID:NOT_FOUND; http://dx.doi.org/10.1134/S1990519X10010050

53 Pelletier J, Sonenberg N. The involvement of mRNA secondary structure in protein synthesis. Biochem Cell Biol 1987; 65:576–81; PMID:3322328; http://dx.doi.org/10.1139/o87-074

54 Calvo SE, Pagliarini DJ, Mootha VK. Upstream open reading frames cause widespread reduction of protein expression and are polymorphic among humans. Proc Natl Acad Sci U S A 2009; 106:7507–12; PMID:19372376; http://dx.doi.org/10.1073/pnas.0810916106

55 Hughes TA. Regulation of gene expression by alternative untranslated regions. Trends Genet 2006; 22:119–22; PMID:16430990; http://dx.doi.org/10.1016/j.tig.2006.01.001

56 Pesole G, Mignone F, Gissi C, Grillo G, Licciulli F, Liuni S. Structural and functional features of eukaryotic mRNA untranslated regions. Gene 2001; 276:73–81; PMID:11591473; http://dx.doi.org/10.1016/S0378-1119(01)00674-6

57 López-Lastra M, Rivas A, Barría MI. Protein synthesis in eukaryotes: the growing biological relevance of cap-independent translation initiation. Biol Res 2005; 38:121–46; PMID:16238092

58 Pisarev A V, Shirokikh NE, Hellen CUT. Translation initiation by factor-independent binding of eukaryotic ribosomes to internal ribosomal entry sites. C R Biol 2005; 328:589–605; PMID:15992743; http://dx.doi.org/10.1016/j.crvi.2005.02.004

59 Jackson RJ. The current status of vertebrate cellular mRNA IRESs. Cold Spring Harb Perspect Biol 2013; 5; PMID:23378589; http://dx.doi.org/10.1101/cshperspect.a011569

60 Gilbert WV. Alternative ways to think about cellular internal ribosome entry. J Biol Chem 2010; 285:29033–8; PMID:20576611; http://dx.doi.org/10.1074/jbc.R110.150532

61 Ozretić P, Bisio A, Inga A, Levanat S. The growing relevance of cap-independent translation initiation in cancer-related genes. Period Biol 2012; 114:471–8

62 King HA, Cobbold LC, Willis AE. The role of IRES trans-acting factors in regulating translation initiation. Biochem Soc Trans 2010; 38:1581–6;

PMID:21118130; http://dx.doi.org/10.1042/BST0381581

63 Mokrejs M, Masek T, Vopálensky V, Hlubucek P, Delbos P, Pospísek M. IRESite–a tool for the examination of viral and cellular internal ribosome entry sites. Nucleic Acids Res 2010; 38:D131–6; PMID:19917642; http://dx.doi.org/10.1093/nar/gkp981

64 Chiang PW, Carpenter LE, Hagerman PJ. The 5'-untranslated region of the FMR1 message facilitates translation by internal ribosome entry. J Biol Chem 2001; 276:37916–21; PMID:11489899; http://dx.doi.org/10.1074/jbc.M101219200

65 Sehgal A, Briggs J, Rinehart-Kim J, Basso J, Bos TJ. The chicken c-Jun 5' untranslated region directs translation by internal initiation. Oncogene 2000; 19:2836–45; PMID:10851087; http://dx.doi.org/10.1038/sj.onc.1203601

66 Pyronnet S, Pradayrol L, Sonenberg N. A cell cycle-dependent internal ribosome entry site. Mol Cell 2000; 5:607–16; PMID:10882097; http://dx.doi.org/10.1016/S1097-2765(00)80240-3

67 Sherrill KW, Byrd MP, Van Eden ME, Lloyd RE. BCL-2 translation is mediated via internal ribosome entry during cell stress. J Biol Chem 2004; 279:29066–74; PMID:15123638; http://dx.doi.org/10.1074/jbc.M402727200

68 Coldwell MJ, deSchoolmeester ML, Fraser GA, Pickering BM, Packham G, Willis AE. The p36 isoform of BAG-1 is translated by internal ribosome entry following heat shock. Oncogene 2001; 20:4095–100; PMID:11494137; http://dx.doi.org/10.1038/sj.onc.1204547

69 Thomas JD, Johannes GJ. Identification of mRNAs that continue to associate with polysomes during hypoxia. RNA 2007; 13:1116–31; PMID:17488873; http://dx.doi.org/10.1261/rna.534807

70 Brahimi-Horn MC, Chiche J, Pouysségur J. Hypoxia and cancer. J Mol Med (Berl) 2007; 85:1301–7; PMID:18026916; http://dx.doi.org/10.1007/s00109-007-0281-3

71 Pan JY, Zhou SH. The hedgehog signaling pathway, a new therapeutic target for treatment of ischemic heart disease. Pharmazie 2012; 67:475–81; PMID:22822532

72 Davuluri R V, Suzuki Y, Sugano S, Zhang MQ. CART classification of human 5' UTR sequences. Genome Res 2000; 10:1807–16; PMID:11076865; http://dx.doi.org/10.1101/gr.GR-1460R

73 Cvok ML, Cretnik M, Musani V, Ozretic P, Levanat S. New sequence variants in BRCA1 and BRCA2 genes detected by high-resolution melting analysis in an elderly healthy female population in Croatia. Clin Chem Lab Med 2008; 46:1376–83; PMID:18844490; http://dx.doi.org/10.1515/CCLM.2008.307

74 Van Eden ME, Byrd MP, Sherrill KW, Lloyd RE. Demonstrating internal ribosome entry sites in eukaryotic mRNAs using stringent RNA test procedures. RNA 2004; 10:720–30; PMID:15037781; http://dx.doi.org/10.1261/rna.5225204

75 Grillo G, Turi A, Licciulli F, Mignone F, Liuni S, Banfi S, Gennarino VA, Horner DS, Pavesi G, Picardi E, et al. UTRdb and UTRsite (RELEASE 2010): a collection of sequences and regulatory motifs of the untranslated regions of eukaryotic mRNAs. Nucleic Acids Res 2010; 38:D75–80; PMID:19880380; http://dx.doi.org/10.1093/nar/gkp902

76 Kasper M, Regl G, Frischauf A-M, Aberger F. GLI transcription factors: mediators of oncogenic Hedgehog signalling. Eur J Cancer 2006; 42:437–45; PMID:16406505; http://dx.doi.org/10.1016/j.ejca.2005.08.039

77 Zaccara S, Tebaldi T, Pederiva C, Ciribilli Y, Bisio A, Inga A. p53-directed translational control can shape and expand the universe of p53 target genes. Cell Death Differ 2014; 21:1522–34; PMID:24926617; http://dx.doi.org/10.1038/cdd.2014.79